CENTRIFUGAL PUMP VIBRATION CAUSED BY SUPERSYNCHRONOUS SHAFT INSTABILITY USE OF PUMPOUT VANES TO INCREASE PUMP SHAFT STABILITY

by

Donald R. Smith

Senior Staff Engineer

Stephen M. Price

Senior Project Engineer

Engineering Dynamics Incorporated

San Antonio, Texas

and

Friedrich K. Kunz

Manager of Engineering

Goulds Pump Municipal Business Unit

Baldwinsville, New York

Donald R. Smith is a Senior Project Leader at Engineering Dynamics Incorporated (EDI). For the past 25 years, he has been active in the field engineering services, specializing in the analysis of vibration, pulsation, and noise problems with rotating and reciprocating equipment. He has authored and presented several technical papers. Prior to joining EDI, he worked at Southwest Research Institute for 15 years as a Senior Research Scientist, where he was also involved in troubleshooting and failure analysis of piping and machinery. Mr. Smith received his B.S. (Physics) from Trinity University (1969). He is a member of ASME and the Vibration Institute.

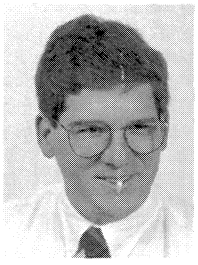

Stephen Price is a Project Engineer for Engineering Dynamics Incorporated. He is actively involved in solving a variety of problems in systems that have experienced failures due to dynamic phenomenon. He has had field and analytical experience solving problems with reciprocating and rotating machinery, along with structural and acoustical problems. Additionally, Mr. Price has been involved in development of multiple channel data acquisition and monitoring hardware and software for critical environments. He has presented and published several papers in the areas of signal processing, finite element analysis, acoustics, and reciprocating pumps. Mr. Price, a registered Professional Engineer and a member of ASME, has a B.S. (Mechanical Engineering) degree from Mississippi State University and an M.S. (Mechanical Engineering) degree from Purdue University.

Friedrich Kunz is Manager of Engineering for the Municipal Business Unit of Goulds Pumps Inc., located in Baldwinsville, New York. His major responsibility is the mechanical design and improvements to existing pump models. In his 29 years in the pump business, he encountered and solved many vibration problems. He graduated from Rudolf Diesel Polytechnikum, Augsburg, Germany, with a B.S. degree (Mechanical Engineering).

ABSTRACT

Many centrifugal pump vibration problems are due to synchronous phenomena such as vane-pass frequency energy and running speed energy. To address such problems, guidelines have been developed to assist with their identification and to evaluate their severity. However, nonsynchronous phenomenon such as recirculation, stage-stall, and shaft instabilities can also cause vibration problems. These types of problems are more difficult to diagnose, since the excitation mechanisms are less obvious. Discussed herein are field measurements and computer analysis that were done to analyze and solve supersynchronous shaft vibration problems on a two-stage horizontal centrifugal coke crusher pump and a vertical single-stage centrifugal water pump. These pumps were marginally stable at low discharge pressures, but were unstable at high discharge pressures. Field tests indicated that the shaft instability vibrations of both pumps could be removed by installing vanes on the back side of the impellers ("pumpout" vanes). Although the pumpout vanes were very effective in eliminating the destabilizing forces on these pumps, the exact effects of the pumpout vanes on the rotor instabilities are not clearly understood. The authors feel that additional analytical and experimental work should be conducted to fully understand the effects of the pumpout vanes.

PUMPOUT VANES

The head or pressure generated by the rotating element in centrifugal pumps, acts on all surfaces in contact with the liquid and generally results in axial and radial thrusts [1, 2]. One method to reduce axial thrust is to cast ribs on the back of the impeller shroud (Figure 1). These ribs are often referred to by many different names, including: "balancing ribs," "radial back vanes," "expeller vanes," and "pumpout vanes." These ribs cause the liquid to rotate at approximately full impeller angular velocity, thus reducing the pressure on the impeller back shroud over the area of the rib [3]. This method of thrust balance is not very accurate or positive and is sensitive to the clearances between the ribs and the case. In addition to thrust balancing, these vanes are widely used in slurry pumps to remove abrasive solids from the seal areas.

The following sections discuss two case histories where pumpout vanes were used to solve supersynchronous shaft instability vibration problems on a horizontal centrifugal pump and a large vertical centrifugal pump.

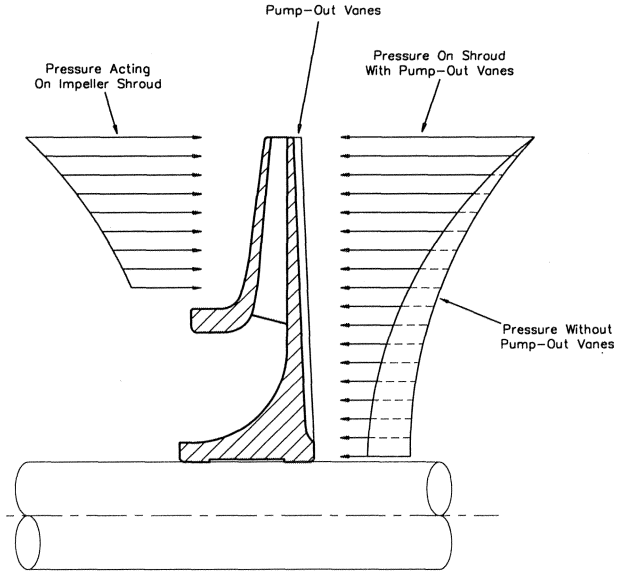

Figure 1. Pumpout Vanes used in a Single-Suction Impeller to Reduce Axial Thrust.

CASE I: TWO-STAGE HORIZONTAL COKE CRUSHER PUMP

Background

A two-stage centrifugal slurry pump with open (unshrouded) impellers (Figures 2 and 3) was to be installed in a refinery as a coke crusher pump. The pump performance data are shown in Table 1.

Table 1. Case I–Pump Performance Data.

Pump Type: 4×6×15 HOS	Speed: 3570 rpm
Design Flow: 648 gpm	TDH: 1670 ft
Suction Pressure: 20 psig	BHP: 552 Max

During shop acceptance tests with the pump operating on water, the pump rotor experienced excessive shaft vibration levels resulting in contact with stationary parts, particularly on the inboard bearing housing seal and the center bushing. Although the pump operated at 3600 rpm, the predominant shaft vibration frequency was approximately 4800 cpm (1.3× running speed). These excessive vibration levels were unusual, because the pump manufacturer had installed many similar coke crusher pumps that operated satisfactorily with no unusual vibration problems.

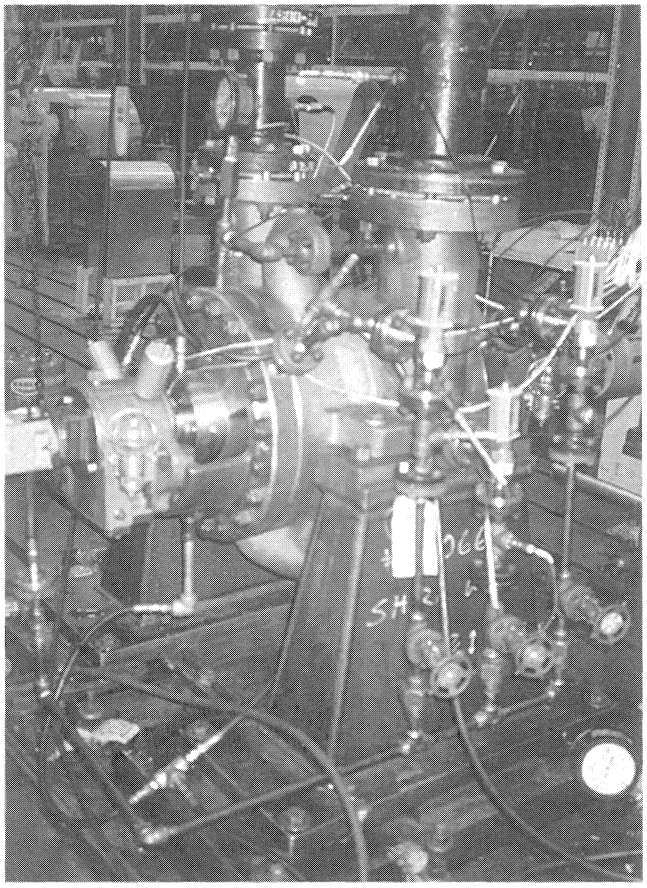

Figure 2. Pump Instrumented During Shop Testing.

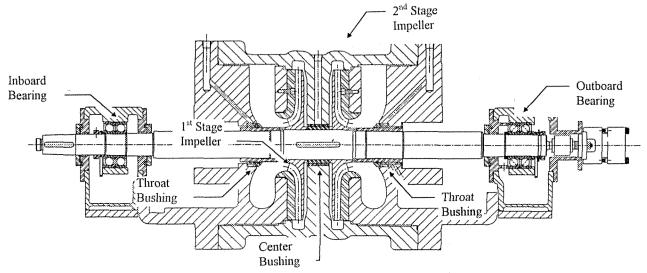

Figure 3. Pump Cross Section.

The pumps were normally supplied with smooth seals (bushings) for the center bushing between the impellers and for the throat bushings at each impeller. The pumps which experienced the problems on the test stand had circular grooved-rotor/smooth-stator seals (Figure 13) which were designed to reduce the leakage and to prevent the coke particles from entering the seals. The analytical rotor stability analysis discussed herein revealed that the grooved seals were destabilizing and caused the shaft to have excessive vibration at 1.3× running speed. It was later determined that the grooved seals were the primary difference between the pumps that had the vibration problem, and the other pumps that had operated satisfactorily for many years.

Impact Testing to Measure the Rotor Mechanical Natural Frequencies

In an effort to determine the cause of the vibration at 1.3× running speed, the pump manufacturer conducted impact tests on the rotor to measure the "dry" rotor lateral natural frequencies. The rotor was removed from the case and mounted on a balance stand. The impact tests indicated a significant response near 1.5× running speed which was excited by impacting one of the impellers in the axial direction (parallel to the shaft). Since the response was excited by impacting the impeller, it was assumed that the measured response was a mechanical natural frequency of the impeller, such as an umbrella mode. However, later computer analysis revealed that the response near 1.5× running speed was actually the first lateral natural frequency of the pump rotor, and not a natural frequency of the impeller.

Effect of Added Stiffener Vanes

The pump manufacturer felt that the response measured during the impact tests could have been the cause of the excessive vibration levels. Therefore, in an attempt to raise the mechanical natural frequency of the impeller further above the running speed, five stiffener vanes were welded to the back side of the impellers (Figure 4). When the pump was tested with the modified impellers, the excessive vibration levels at 1.3× running speed were not present.

Since the temporary stiffener vanes had been effective in eliminating the excessive vibration at 1.3× running speed, the pump manufacturer fabricated new impellers with similar stiffener vanes and a thicker back plate. However, when the pump was run with the modified impellers, the shaft vibration levels were again excessive at 1.3× running speed.

Next, it was decided to perform the previous test again to determine if the data were repeatable. The new impellers were removed and replaced with the previously modified impellers with the five stiffening vanes. When the pump was retested, the vibration levels at 1.3× were not present, which confirmed the earlier test results.

These tests indicated that the pump rotor stability was sensitive to the modifications on the back side of the impellers. It was felt that the stiffening vanes acted as pumpout vanes, which reduced the pressure drop across the center bushing, and may have also reduced the destabilizing (aerodynamic) loading on the impeller blades. It is difficult to evaluate the differences between the original impellers with the stiffening vanes, and the redesigned impellers that also had stiffening vanes. One possible difference between the impellers was the welding of the vanes to the back side of the impellers (Figure 4). The vanes on the original impellers were simply tack welded resulting in a sharp angle between the vane and the impeller. The vanes on the redesigned impellers had full bead welds on both sides of the vanes resulting in a smooth fillet on each side of the vanes. Because of the sharp angle at the side of the vanes, the tack welded vanes may have been more efficient as pumpout vanes compared to the vanes with the full welds.

Stability Analysis

The pump manufacturer requested that vibration analysts assist them in determining the cause(s) of the excessive vibration levels and in developing modifications to reduce the vibration levels. Based upon the vibration characteristics (Figure 5), the vibration analysts felt that the excessive vibration levels at 1.3× running speed were primarily caused by a rotor instability problem. It was recommended that additional vibration and pulsation data be obtained to determine if the problem was related to a self-excited vibration, or a forced vibration caused by excessive pulsation forces [4].

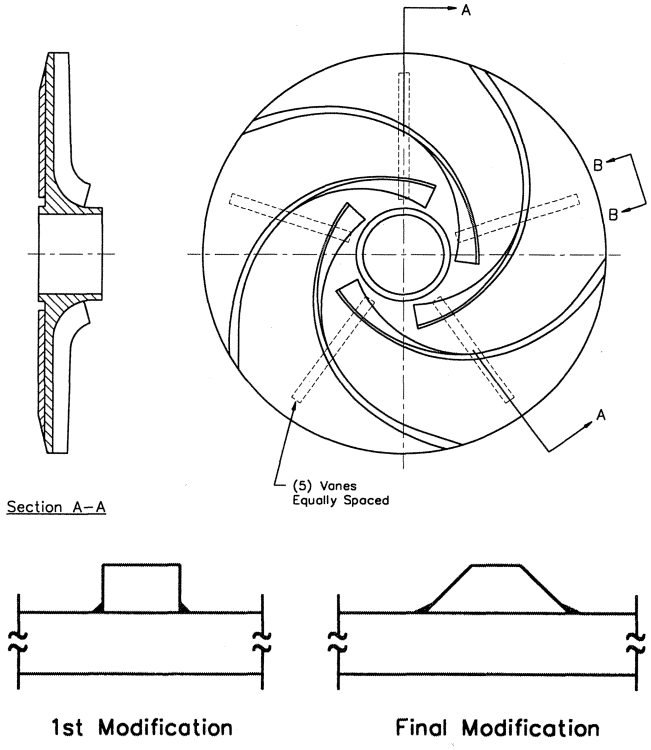

Figure 4. Pump Impeller Illustrating the Stiffener Vanes.

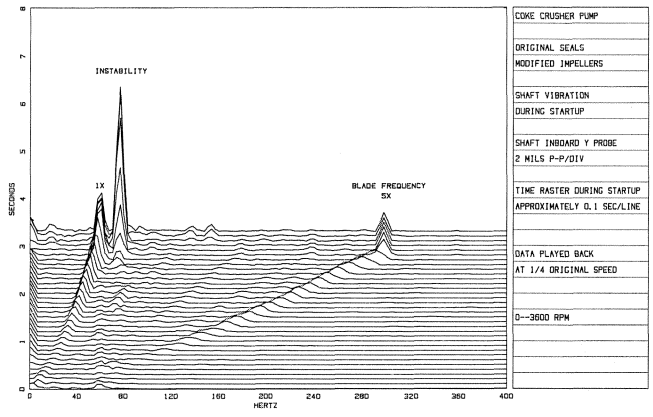

Figure 5. Shaft Instability Vibration During Startup–Original Bushings.

Proximity probes were temporarily installed near the bearings to measure the shaft vibration. Pulsation was measured with piezoelectric dynamic pressure transducers installed in the available pressure tap locations in the suction and discharge piping near the pump, and in the seal flush lines to the center bushing and throat bushings.

The pump is driven by an electric motor which accelerates the pump to full speed in less than 3.0 seconds, which makes it difficult to analyze the vibration data during the startup. To increase the

analysis time, the startup data were tape recorded and played back at 1/4 tape speed. Typical shaft vibration data measured during a startup are shown in Figure 5. During the startup, the shaft vibrations were primarily at 1× running speed and at the blade passing frequency (5× running speed). The shaft vibration data indicated that the instability did not occur until after the pump reached full speed and the discharge pressure was increased, Figure 6.

The vibration data indicated that the rotor was unstable and whirled in a forward precession at certain operating conditions away from the best efficiency point (high pressure and low flow, and reduced pressure and high flow). A plot of the shaft vibration is shown in Figure 7 as the discharge pressure was reduced while the pump operated at a constant speed. As shown, the vibration levels increased when the pump was operated at conditions away from the bep (best efficiency point). Frequency analysis of the vibration data (Figure 8) revealed that the increased vibration levels were caused by the shaft vibration at the instability frequency near 1.3× running speed.

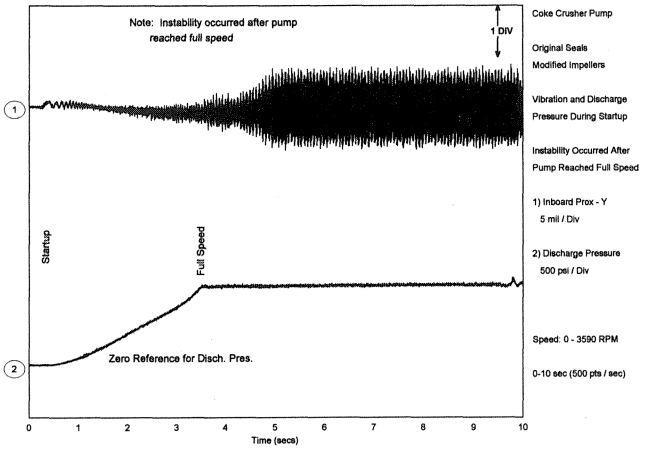

Figure 6. Shaft Vibration (Original Bushings) and Discharge Pressure During Startup.

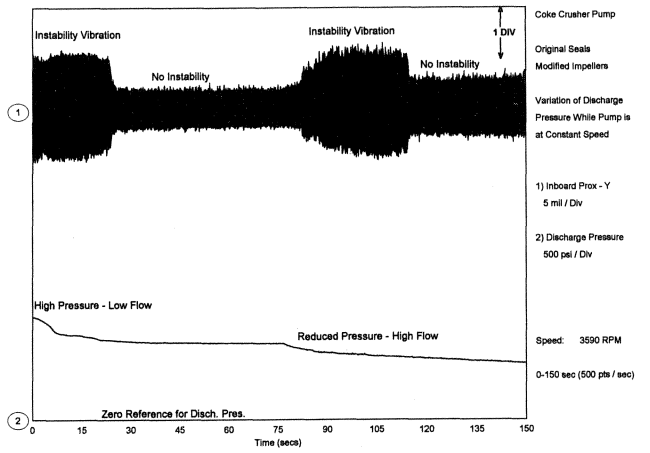

Figure 7. Shaft Instability Vibration (Original Bushings) vs *Pump Discharge Pressure.*

The pulsation data measured in the center bushing (Figure 9) correlated well with the shaft instability vibration. It is difficult to determine if the vibration at the instability frequency was caused by the pulsation at that frequency, or vice versa. Previous experience by the authors has shown that vibration by the shaft and pump impellers can generate pulsation at the vibration frequency. As discussed below, it was later determined that the vibrations at 1.3× running speed were due to the self-excited rotor instability. Therefore, it was felt that the pulsation at the instability frequency was a result of the shaft vibration, rather than the cause of the shaft vibration.

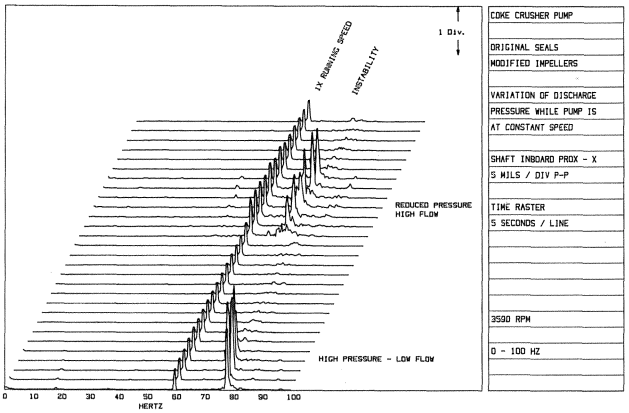

Figure 8. Frequency Spectra of Shaft Vibration vs *Pump Discharge Pressure.*

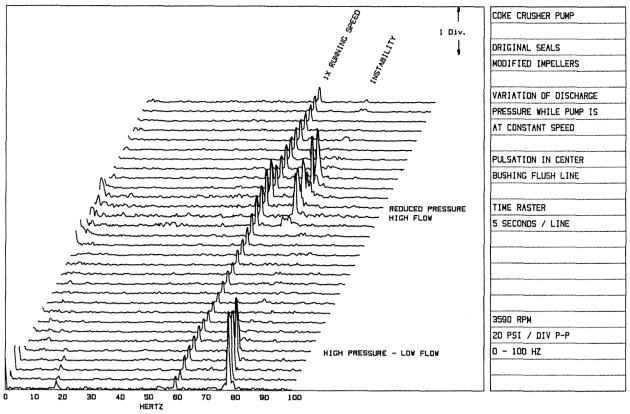

Figure 9. Frequency Spectra of Pulsation in Center Bushing Flush Line vs *Pump Discharge Pressure with Original Bushings.*

In the case of self-excited rotordynamic instabilities, the rotor generally whirls at a frequency near a rotor lateral natural frequency. For rotors that operate above the first lateral natural frequency, the instability vibration will be subsynchronous (below the running speed). Similarly, for rotors operating below the first lateral natural frequency, such as this coke crusher pump, the instability vibration will be supersynchronous (above the running speed). Subsynchronous instabilities are fairly common; however, supersynchronous instabilities are very rare. In fact, many people feel that rotor instabilities will not occur if the rotor first lateral natural frequency is above the running speed.

The instability vibrations are self-excited and the vibration levels can rapidly increase until some nonlinear effect limits further increase, or until the rotor contacts a stationary part (such as the center bushing and seals). In the case of the pump, the energy supplying the instability vibrations was related to the differential loading on the pump impeller blades. The differential loading creates destabilizing cross coupling forces that induce whirl in the direction of rotation. These forces produce cross coupled stiffness coefficients (K_{xy}) that were first identified in axial-flow turbomachinery [5]. As shown below, the equation for estimating the cross coupling coefficients was later modified for use with centrifugal compressors [6].

$$K_{yx} = \frac{-6300\ (\mathrm{HP})\ (\mathrm{MW})}{N\ D\ h}\ \frac{\rho_d}{\rho_s} \qquad (1)$$

where:

HP = horsepower
MW = molecular weight
ρ_d = discharge density
ρ_s = suction density
N = speed, rpm
D = impeller diameter
h = minimum restrictive dimension in flow path

This equation can also be modified for application to centrifugal pumps. Since the forces were originally applied to turbines and compressors, the loading is generally referred to as "aerodynamic" loading. Therefore, the term aerodynamic loading is also used when dealing with pumps, even though the operating fluid is a liquid and not a gas. The aerodynamic cross coupling (K_{xy}) for pumps can be estimated using the following equation.

$$K_{yx} = \frac{\text{-6300 (HP)}}{N\ D\ h} \tag{2}$$

Basic Concepts of Rotor Stability

Self-excited rotor vibration or instability can be thought of as free vibration of a system having negative damping. In a system with positive damping, free vibrations decay when the exciting force is removed. In a system with negative damping, when a perturbation initiates the vibration, it grows without bound [7]. These concepts are illustrated in Figure 10.

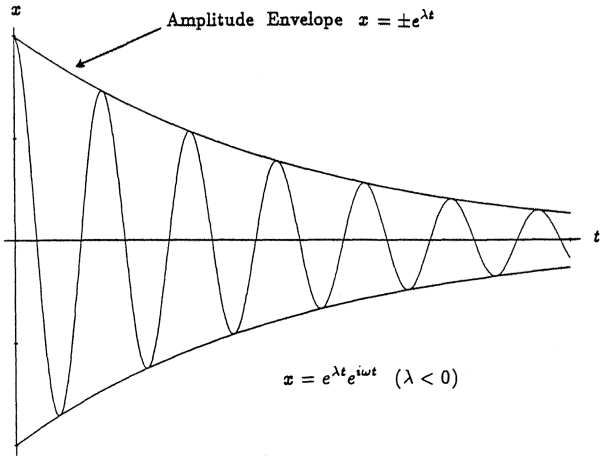

(a) Stable System

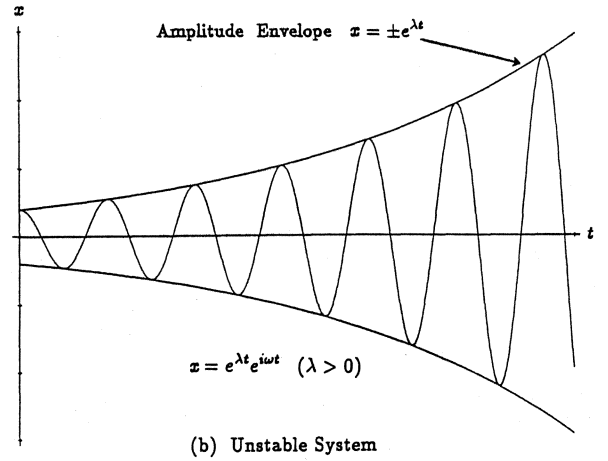

(b) Unstable System

Figure 10. Comparison of Stable and Unstable Systems.

Instability can be demonstrated mathematically using a single degree of freedom model. The differential equation of motion for such a system is:

$$m\ddot{x} + c\dot{x} + kx = 0 \tag{3}$$

where

k = stiffness
c = damping constant
m = mass
x = displacement

The solution to this equation is

$$x = e^{-(\frac{c}{2m})t}\, e^{i\omega t} \tag{4}$$

or

$$x = e^{-(\frac{c}{2m})t}\, (A \cos\omega t + B \sin\omega t) \tag{5}$$

Damping in the system can be evaluated by comparing the amplitudes of vibration x_1 and x_2 occurring n cycles apart at times t_1 and t_1 [8]. This ratio reduces to

$$\frac{x_2}{x_1} = e^{-(\frac{c}{2m})t} \tag{6}$$

Note that if the quantity

$$e^{-(\frac{c}{2m})t} > 1 \tag{7}$$

the vibrations will increase with time as shown above.

Therefore if $\frac{-ct}{2m} > 0$, the vibrations will be unstable. For convenience, the quantity $\frac{-c}{2m}$ is defined as λ, the growth factor.

The logarithmic decrement (log dec) is defined as

$$\delta = \frac{1}{n} \ln\left(\frac{x_2}{x_1}\right) = \frac{2\pi\zeta}{\sqrt{1-\zeta^2}} \tag{8}$$

where ζ is the viscous damping factor and is defined by

$$\zeta = \frac{c}{2m\omega_n} \tag{9}$$

For small ζ, then

$$\delta \approx 2\pi\zeta \tag{10}$$

Therefore, the log dec can be written

$$\delta \approx 2\pi\zeta = \frac{-2\pi\lambda}{\omega_n} = -\frac{\lambda}{f} \tag{11}$$

This is a convenient form of the logarithmic decrement relationship since the eigenvalues for the damped critical speeds are of the form:

$$s = \lambda + i\omega \tag{12}$$

where:

ω = whirl frequency, radians/sec
λ = growth factor, l/sec

Since ω is positive, a stable vibration ($\lambda < 0$) has a positive log decrement. Theoretically, rotors with log dec values greater than zero are stable. However, to ensure that the rotor remains stable

under actual operating conditions, the log dec should be approximately 0.3 for the complete rotor with all of the seal (bushing) effects determined at the full load condition (full aerodynamic loading). For log dec values between 0 and +0.3, the rotor is considered marginally stable.

Rotor Stability Analysis

An assessment of the rotor stability was made with a computer program utilizing a modified Myklestad-Prohl procedure that computes the damped eigenvalues and the growth factors.

Effective Bearing Stiffness

The rotor was modelled as shown in Figure 11. The pump has rolling element bearings that are supported by the bearing housings. The effective stiffness of the bearings was not known; therefore, the undamped rotor lateral natural frequencies were computed for a large range of bearing stiffnesses and are plotted on the critical speed map (Figure 12). These frequencies were computed for the "dry" rotor simply supported at the bearings without the center bushing and throat bushings. This would be similar to the rotor mounted on the balance stand.

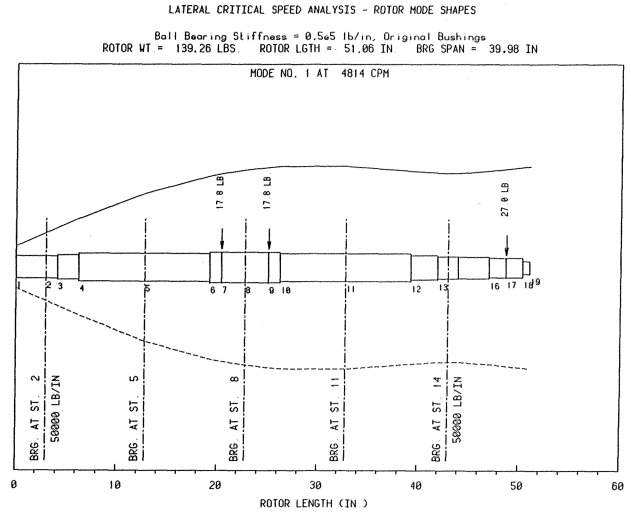

Figure 11. Pump Rotor Model and Vibration Mode Shape.

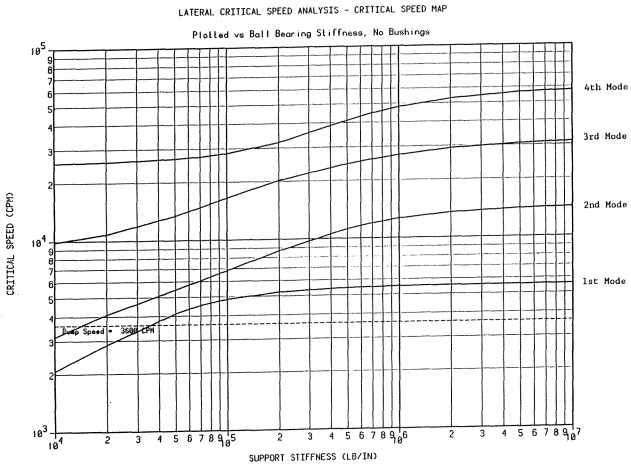

Figure 12. Lateral Critical Speed Map.

When the rotor lateral natural frequencies were computed using typical stiffness values for the rolling element bearings of 500,000 to 1,000,000 lb/in, the lateral natural frequencies were significantly larger than those measured in the field. It was determined that the computed instability frequencies had good agreement with the measured frequencies when the bearing stiffnesses were reduced to 50,000 lb/in It is felt that the effective stiffnesses were lowered, due to the combined effects of the flexibility of the bearing housings, clearance between the bearing outer shell and the bearing housing, and the flexibility of the bearing support inside the bearing housing.

Using a bearing stiffness of 50,000 lb/in, the dry rotor first lateral natural frequency without bushings was computed to be 4120 cpm (approximately 1.14× running speed), Figure 12. This lateral natural frequency was lower than the value measured during the impact tests on the balance stand because the effective support stiffness was probably larger on the balance stand.

The calculated rotor first lateral natural frequency was increased to approximately 4,800 cpm (1.3× running speed) when the throat and center bushing stiffnesses were included in the model at stations 5, 8, and 14, Figure 11. This "wet" lateral natural frequency generally agreed with the frequency of the supersynchronous vibration. The vibration mode shape indicated higher amplitudes on the coupling side of the inboard bearing (Station 13) that agreed with the field data and the location of some of the previous rubs.

Stiffness and Damping Coefficients for the Bushings

At high discharge pressures, the flow of liquid through the bushings create a hydrodynamic bearing effect, which transforms the rotor from one supported at two bearings external to the pump to one with three additional internal bearings lubricated by the pumped liquid. Each of the bearings and bushings were modelled using four stiffness coefficients (K_{xx}, K_{xy}, K_{yx}, K_{yy}) and four damping coefficients (C_{xx}, C_{xy}, C_{yx}, C_{yy}) an outside company was contracted to compute the coefficients for the bushings.

Analysis of the Grooved Seals

The pump configuration that experienced the instability problems had circular grooved-rotor/smooth-stator seals for both the center and throttle bushings, Figures (13, 14, 15 and 16). The geometries of the center and throttle bushings are shown in Table 2. The computer stability analysis were performed for the condition on the test stand with water and for the field conditions with the hydrocarbons. The operating conditions for both are shown in Table 3. The computer model did not include the effects of the pumpout vanes, because the exact effects of the pumpout vanes were unknown.

Table 2. Grooved Seal Geometry.

Parameter	Center Bushing	Throttle Bushing
Seal Length	0.625 in	0.625 in
Seal Diameter	3.767 in	3.500 in
Groove Width	0.063 in	0.125 in
Groove Depth	0.050 in	0.050 in
Land Width	0.063 in	0.063 in
Radial Clearance	8–10 mils	15–18.5 mils

Table 3. Pump Seal Parameters.

Parameter	Center Bushing	Throttle Bushing
Pressure Drop	310 psi	346 psi
Shaft Speed	3560 rpm	3560 rpm
Computed Inlet Swirl	0.80	0.50

The analysis of the grooved seal was accomplished using a bulk flow solution for incompressible flow seals which was derived from the work of Scharrer [9]. The results of the analysis are shown in Table 4 for the pump operating with water (H_2O) and hydrocarbon (HC).

Table 4. Grooved Seal Performance.

	K_{xx} lbf/in	K_{xy} lbf/in	C_{xx} lbf-s/in	C_{xy} lbf-s/in	M_{xx} lbm
Center Bushing (H2O)	10,500	11,600	13.0	1.2	1.5
Center Bushing (HC)	8,600	9,600	11.5	1.6	1.5
Throttle Bushing (H2O)	6,100	3,400	7.8	0.7	0.6
Throttle Bushing (HC)	4,800	2,700	7.3	0.5	0.6

$$K_{yy} = K_{xx}, \quad K_{yx} = -K_{xy}, \quad C_{yy} = C_{xx}, \quad C_{yx} = -C_{xy}$$

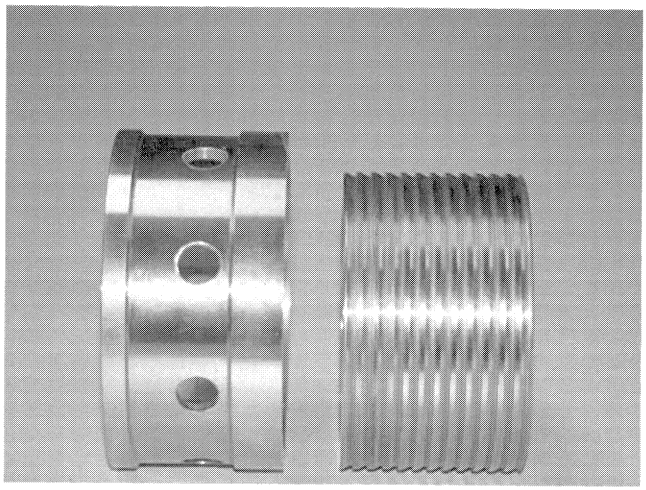

Figure 13. Original Center Bushing.

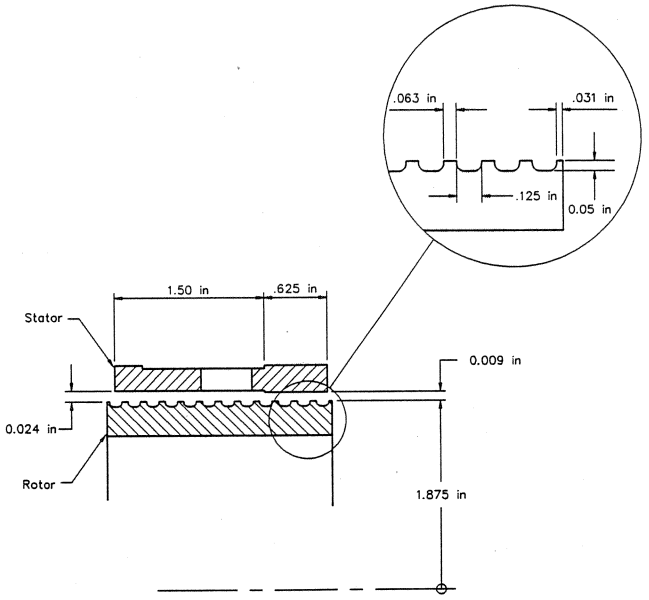

Figure 14. Original Center Bushing (Grooved Stator).

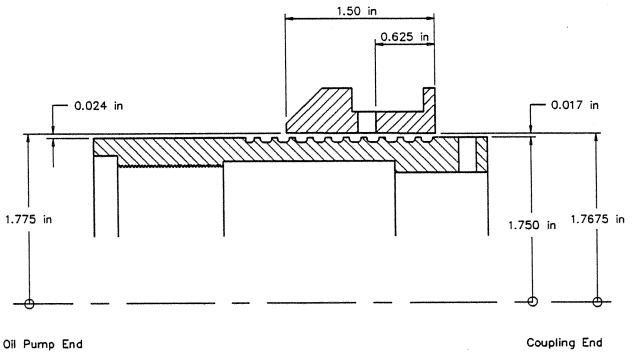

Figure 15. Original Throat Bushing–Coupling End (Grooved Stator).

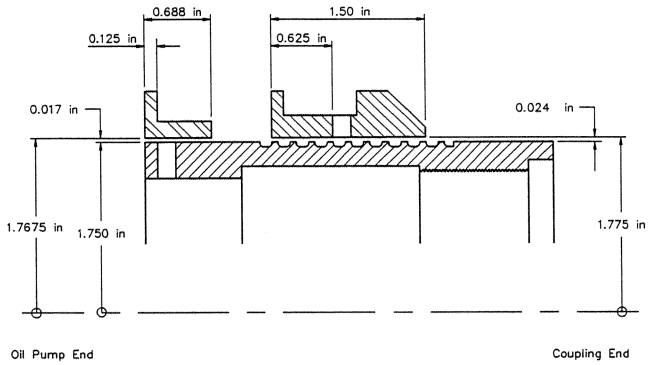

Figure 16. Original Throat Bushing–Oil Pump End (Grooved Stator).

Stability of Original Rotor

The original rotor was modelled as shown in Figure 11, using an effective bearing stiffness of 50,000 lb/in and the seal coefficients for water shown in Table 4. The log dec values were plotted *vs* aerodynamic loading for the forward mode near 4,800 cpm (first damped eigenvalue), Figure 17. The log dec at a low aerodynamic loading of 100 lb/in was approximately 0.1, which is considered to be a low log dec value. As shown, the log dec value was reduced as the aerodynamic loading increased. The log dec became negative (unstable) as the aerodynamic loading increased to approximately 2,000 lb/in.

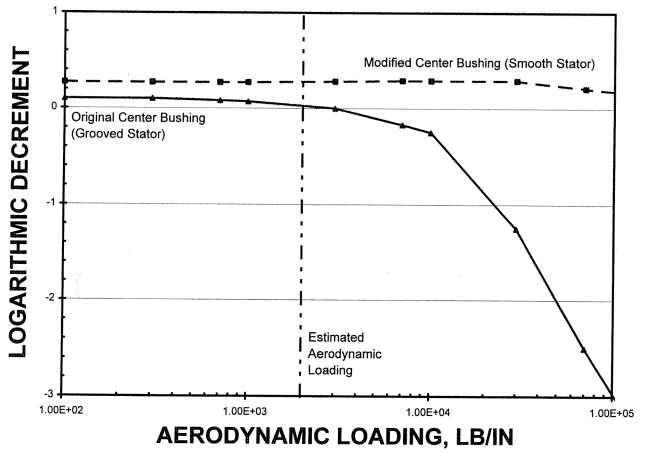

Figure 17. Stability Map–Original Center Bushing and Modified Center Bushing.

The cross coupling loading (K_{yx}) for this pump was estimated to be approximately 1,500 lb/in. This value generally agreed with the computer analysis that showed that the rotor became unstable as the discharge pressure was increased.

Seal Replacement Options

The stability calculations indicated that the center and throttle bushings were destabilizing and caused the rotor to become unstable. The seal calculations indicated that the rotor stability could be significantly improved by modifying the bushings (seals), especially the center bushing. One possible modification to the center bushing was to remove the grooves from the rotating sleeve (rotor) and to maintain the minimum clearance for the entire length of the stationary bushing (stator). The geometry used in the annular seal analysis is shown in Table 5.

Table 5. Annular Seal Geometry.

Parameter	Center Bushing	Throttle Bushing
Seal Length	0.63 in	0.63 in
Seal Diameter	3.767 in	3.50 in
Radial Clearance	8–10 mils	15–18.5 mils

The computed stiffness and damping values for smooth center bushing and smooth throttle bushings are shown in Table 6.

Table 6. Smooth Annular Seal Performance.

	K_{xx} lbf/in	K_{xy} lbf/in	C_{xx} lbf-s/in	C_{xy} lbf-s/in	M_{xx} lbm
Smooth Center Bushing (H2O)	22,500	6,000	19.5	0.7	0.5
Smooth Center Bushing (HC)	19,700	5,900	19.4	0.6	0.4
Smooth Throttle Bushing (H2O)	8,500	2,000	10.8	0.2	0.2
Smooth Throttle Bushing (HC)	6,400	2,000	10.8	0.2	0.2

$$K_{yy} = K_{xx}, \quad K_{yx} = -K_{xy}, \quad C_{yy} = C_{xx}, \quad C_{yx} = -C_{xy}$$

The results shown in Table 6 indicate that the smooth annular seal has half the crosscoupled stiffness and 50 percent more direct damping than the grooved seal.

Rotor Stability with Modified Center Bushing

The computed log decs for the system with the modified center bushing are plotted in Figure 17. The log decs were increased to approximately 0.3 at low aerodynamic loads and remained positive (stable) even at high aerodynamic loads of 100,000 lb/in, which was well above the actual loading value.

Based upon this analysis, the engineering company recommended that the grooves on the center bushing should be removed. To evaluate the effects of the seals on the rotor stability, the rotor was configured with the modified impellers that had previously resulted in the supersynchronous instability. When the rotor was tested with the modified center bushing, the rotor remained stable and the supersynchronous vibration levels were significantly reduced even when the pump was operated near shutoff conditions (Figure 18). Pulsation data measured in the center bushing seal flush line

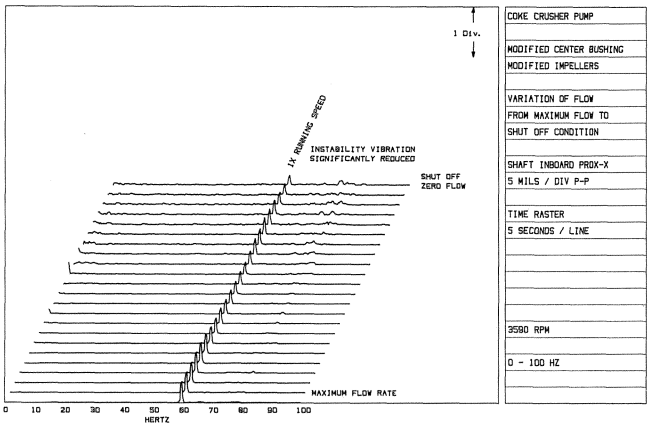

Figure 18. Frequency Spectra of Shaft Vibration (Modified Center Bushing) vs *Pump Operating Conditions.*

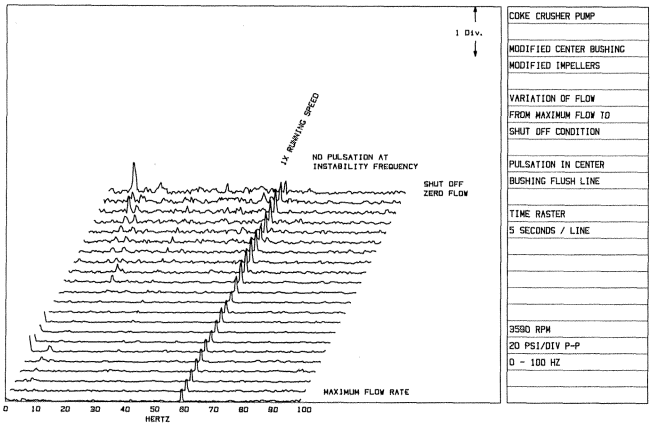

Figure 19. Frequency Spectra of Pulsation in Center Bushing Flush Line with Modified Center Bushing.

(Figure 19) also indicated that the pulsation at the instability frequency was no longer present. The fact that the pulsation was no longer present verified that the pulsation at the instability frequency was caused by the shaft vibration.

To further improve the rotor stability and to reduce the bearing housing vibration, the original grooved throttle bushings were also replaced with smooth seals. It was reported that the pumps were also stable when the pumps were operated with hydrocarbons in the refinery. As shown, the field tests and the computer analysis both indicated that the rotor instability vibration could be reduced by modifying the bushings to improve the rotor stability, or by installing the pumpout vanes to reduce the pressure drop across the center bushing.

CASE II: LARGE VERTICAL SINGLE–STAGE CENTRIFUGAL PUMP

Three single-stage vertical centrifugal pumps were installed in a waste water treatment plant as effluent pumps (Figures 20 and 21). The pump performance data are shown below in Table 7.

Table 7. Case II–Pump Performance Data.

Pump Type: 7100 size 54×54-6	Speed: 300 rpm
Design Flow: 144 mgd	TDH: 59 ft
Number of Impeller Vanes: 4	

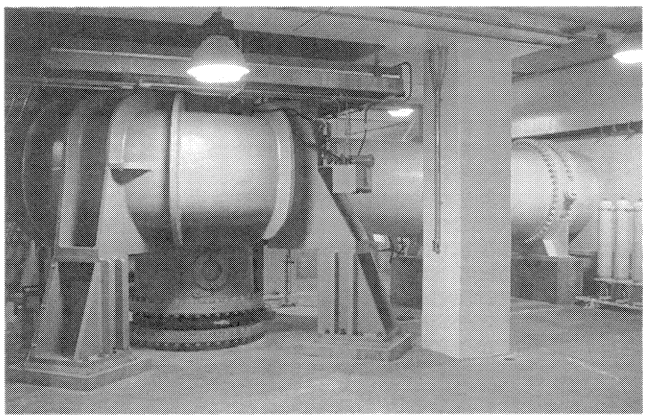

Figure 20. Pump Installation.

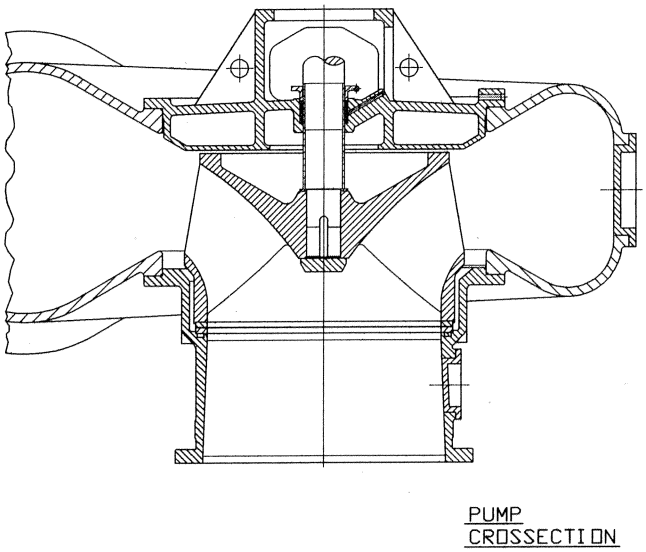

Figure 21. Pump Cross Section.

The three pumps were driven by synchronous electric motors that were controlled with variable frequency drives (VFDs). The pump speed ranged from 150 to 300 rpm. The pumps experienced excessive supersynchronous vibration when they were operated at high speeds with high head pressures. The equipment packager requested that testing be performed to assist them in determining the cause(s) of the vibration problem.

Previous Experience of the Pump Manufacturer

Supersynchronous vibration where the frequency is unaffected by pump speed had not been experienced by the pump manufacturer prior to 1990. Two vertical pumps similar to these were installed at another location where one of the pumps experienced a similar supersynchronous vibration problem. The pump manufacturer conducted tests to determine the cause(s) of the supersynchronous vibration.

An observation was made that pressure pulsation in the casing behind the impeller (the "ring cavity") occurred at the onset of vibration. Based upon this information, the pump manufacturer recommended air injection into the ring cavity to "break up" the pulsation wave. When air was injected, the supersynchronous vibration was immediately reduced. This pump has continued to operate satisfactorily with the air injection.

Field Tests at the Waste Water Treatment Plant

The three pump/piping systems were identical; however, as often happens, the vibration levels were significantly different between the pumps. Pump 2 had the highest vibration levels and was very sensitive to changes in the operating conditions. Pump 1 showed a sensitivity to changes in the operating conditions, but the vibration levels were much lower compared to Pump 2. Pump 3 was not sensitive to operating conditions and could be operated over the entire performance map with low vibration levels. To evaluate the differences between the pumps, field data were obtained on Pumps 2 and 3.

The pumps were instrumented as shown in Figure 22. Vibration measurements on the bearing housing indicated that the vibration levels at the pump running speed and blade-pass frequency were almost nonexistent and that the vibration was predominantly at two supersynchronous frequencies. Shaft vibration data measured with proximity probes showed that the shaft whirled at 6.6 Hz (backward whirl) and 8.6 Hz (forward whirl), depending upon the running speed and pressure ratio (Figure 23).

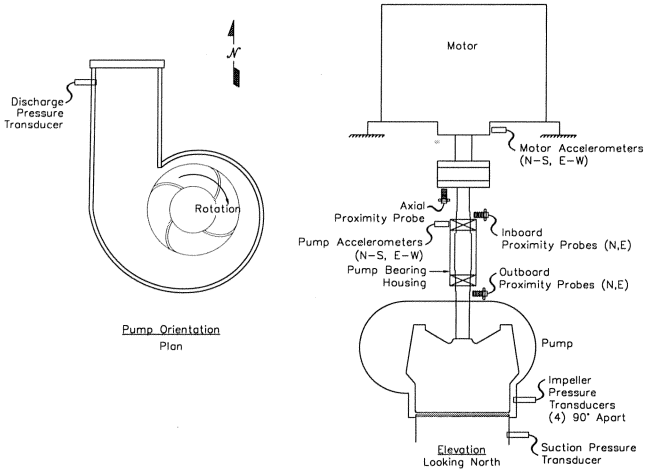

Figure 22. Vibration and Pulsation Transducer Instrumentation.

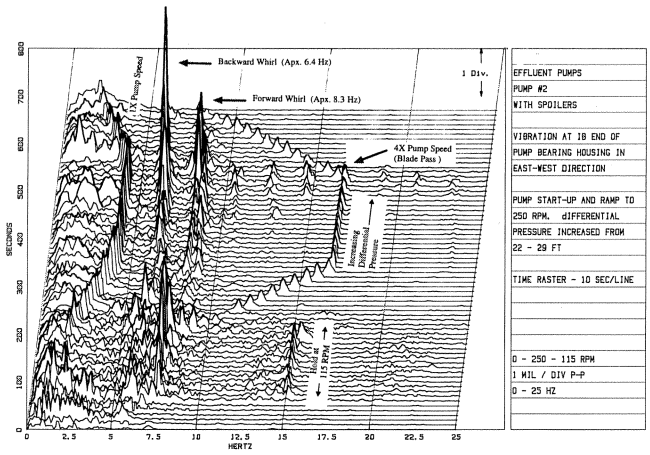

Figure 23. Shaft Instability Vibration with Spoilers Installed.

Since the pump operated slowly, the direction of whirl could be determined by observation of the orbit on an oscilloscope.

Alternatively, the direction of whirl could be determined by comparing the shaft rotation direction with the vibration data (Figure 24). As shown in Figure 25, the 6.5 Hz vibration at the East

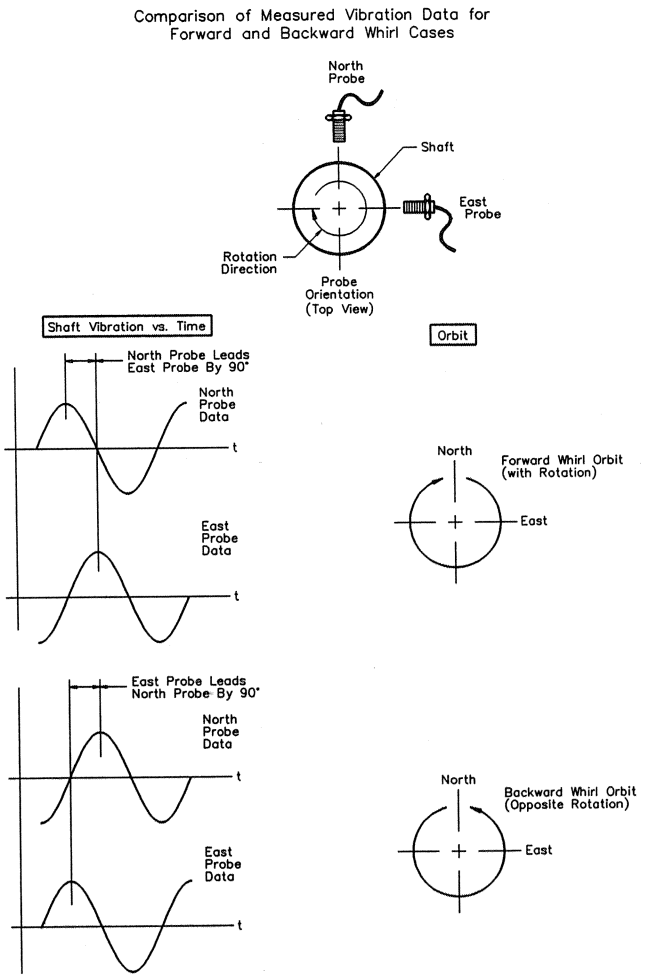

Figure 24. Comparison of Measured Vibration Data for Forward and Backward Whirl Cases.

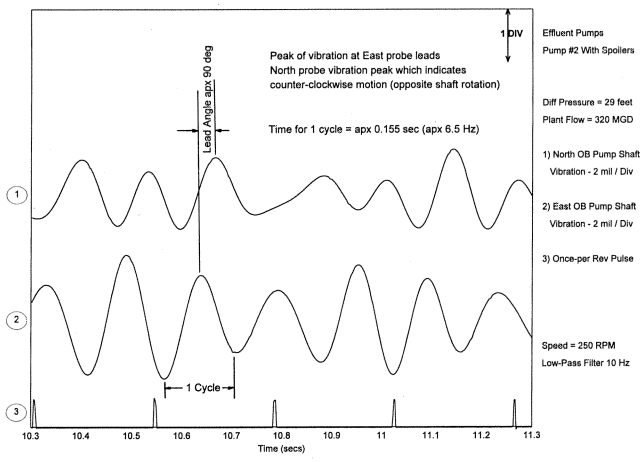

Figure 25. Illustration of Backward Whirl.

probe leads the vibration at the North probe, indicating backwards motion. For vibration at 8.4 Hz, the North probe leads the East probe, indicating forward motion (Figure 26).

Forward Mode

The data indicated that the forward mode near 8 Hz was excited when multiples of the pump running speed were coincident with

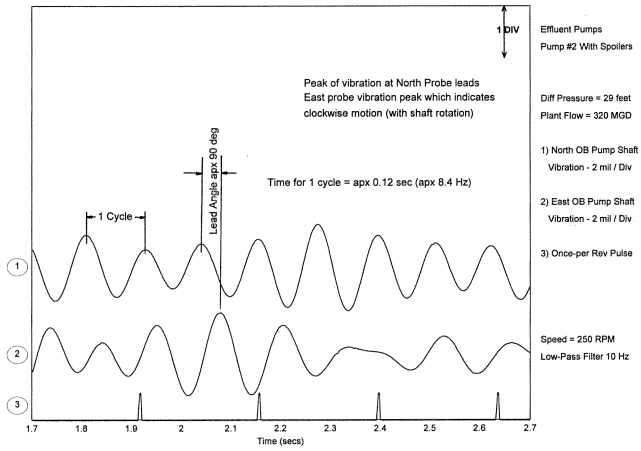

Figure 26. Illustration of Forward Whirl.

that frequency. For example, as shown in Figure 23, the forward mode was excited by pulsation energy at the blade passing frequency (4× running speed) when the pump speed was approximately 120 rpm. The forward mode was also excited by energy at 2× running speed when the pump was running at approximately 250 rpm.

Backward Mode

The backward mode was difficult to excite when the forward mode was being excited at the pump speed of approximately 250 rpm. The data indicated that the rotor would alternate between the forward and backward modes and that neither of the modes was predominant, even at the high differential pressures. At maximum speed, the backward mode near 6.0 Hz was the dominant mode.

Backward modes are usually more difficult to excite than the forward modes. The backward mode near 6.0 Hz mode was excited when the differential pressures were increased above 25 ft. Backward modes can be excited by forces in the direction opposite to normal rotation.

One of the most common sources of backward excitation is a rub with a stationary component. Initially, it was felt that the backward whirl was caused by contact between the rotor and stationary components, such as the wear ring seal. However, inspection of the pump indicated that the rotor had not contacted the seals. In addition, the measured shaft deflection data showed that the vibration levels were highest when the rotor was operating near the center of the bearing clearances. An FEA analysis of the rotor also indicated that the shaft deflections were too low to result in contact with the stationary seals. The fact that the rotor was not rubbing is significant, because most of the literature indicates that it is difficult for a rotor to whirl backwards without contacting a stationary component.

The field tests showed that Pump 3 did not vibrate at the backward mode, even at the high differential pressures. The shaft deflection data acquired during the field tests indicated that the pump rotor deflected considerably more than Pump 2. This increased deflection suggested that the bearing clearances in Pump 3 were much larger compared to Pump 2. It is thought that the increased bearing clearances could have increased the damping that in turn increased the rotor stability, making the rotor less sensitive to the destabilizing forces on the rotor.

Phase-Locked Pulsation

Pulsation data measured in the cavity between the impeller and case showed significant pulsation at the instability frequencies

(Figure 27). The pulsation wave was phase-locked with the shaft whirl direction, whether it was forward or backward (Figure 28). However, the pulsation was not thought to be due to an acoustic resonance, since the dimensions were too small for such acoustical natural frequencies.

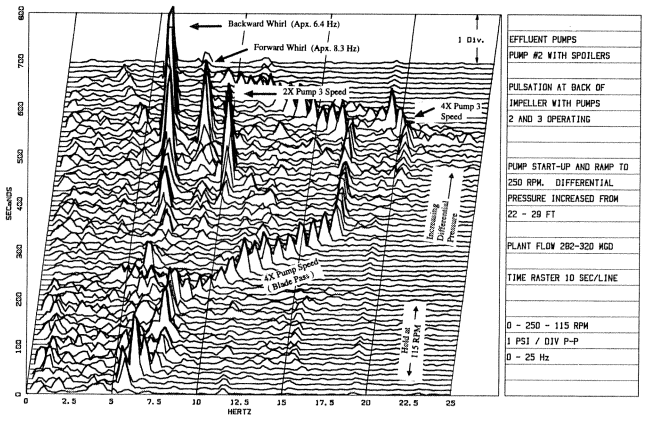

Figure 27. Pulsation Measured Behind Impeller with Spoilers Installed.

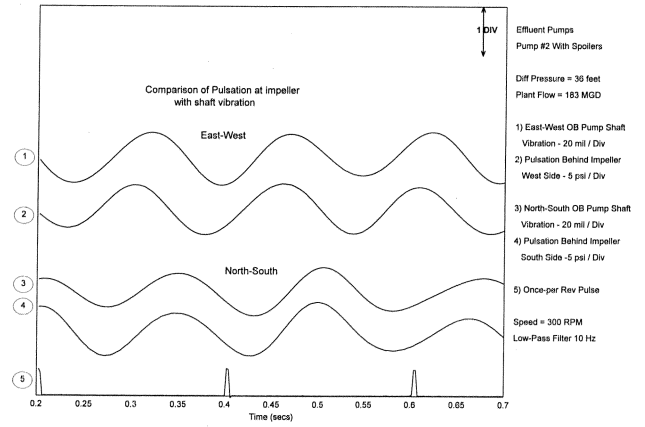

Figure 28. Comparison of Pulsation Behind Impeller with Shaft Vibration.

It was thought that the phase-locked pulsation was due to whirling of the shaft at a self-excited rotor instability. This problem was very similar to that experienced on several vertical-shaft pumps installed at the Dos Amigos pumping station in California [10].

Shaker Tests

In an effort to separate the effects of the pulsation forces and the shaft lateral natural frequencies, shaker tests were conducted on Pump 2. A shaker that provided a rotating force perpendicular to the rotor axis was installed at the lower bearing housing (Figure 29).

The speed of the shaker was varied from 5.0 to 17 Hz to provide energy throughout the range of normal vane-pass excitation. Using this apparatus, several investigations were performed.

First, the shaker was operated with the unit "dry" (i.e., with the water drained). Data were acquired from proximity probes installed at the lower bearing housing. Since there was no water in the pump, an accelerometer was easily attached to the bottom of the impeller to measure the actual displacements of the rotor. This test allowed measurement of the first rotor natural frequency without the effect of the water (for comparison to analytical models).

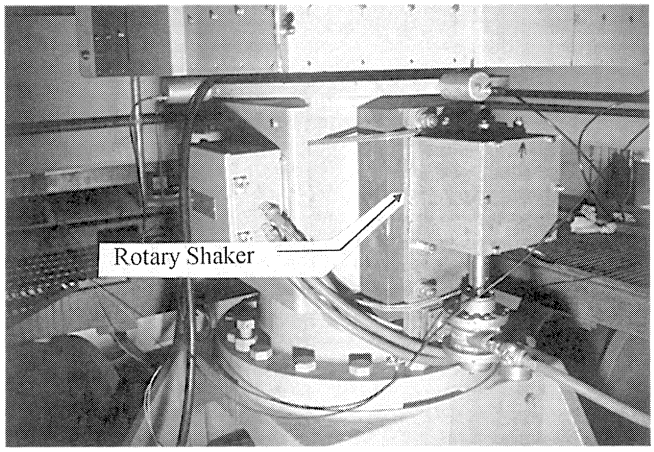

Figure 29. Shaker Installed on Pump Housing.

Also, a relationship between the vibration at the end of the impeller and vibration measured at the proximity probes could be determined. This relationship was later used to estimate the shaft motion at the end of the impeller from proximity probe data acquired when the unit was full of water. As shown in Figure 30, the dry rotor natural frequency was measured to be 12.5 Hz.

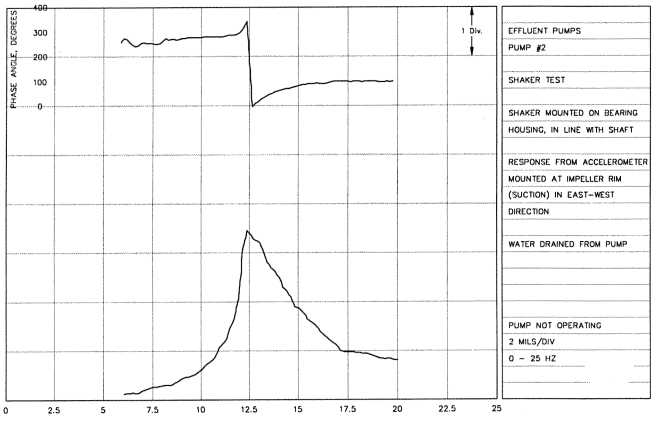

Figure 30. Pump Rotor Dry Natural Frequency During Shaker Test.

After filling the pump with water, the shaker tests were repeated. The data showed that the effective mass of water in the impeller reduced the rotor first natural frequency from 12.5 Hz dry to 8.8 Hz wet (Figure 31). The value of 8.8 Hz agreed favorably with the

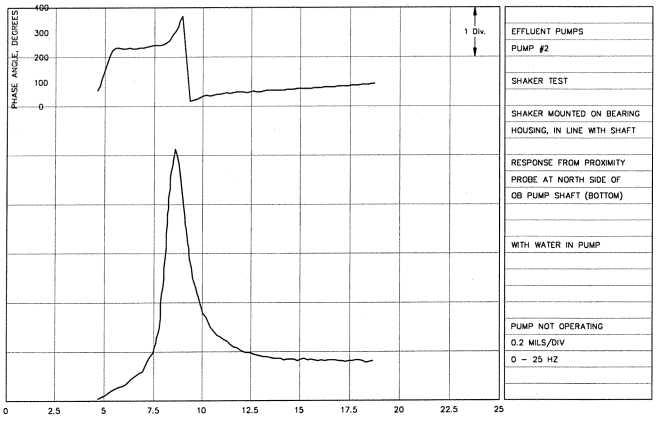

Figure 31. Pump Rotor Wet Natural Frequency During Shaker Test.

forward mode frequency of 8.3 Hz measured with the pump in operation. The backward instability frequency could not be excited with the shaker because when the shaft was at rest, the forward and backward modes would occur at the same frequency. The computer analysis indicated that the backward mode would be lowered from approximately 8.0 Hz to the measured value near 6.0 Hz by the gyroscopic effects when the shaft was rotating.

Pulsation data were measured in the cavity behind the impeller while the shaker was operated. As shown in Figure 32, pulsation measured in the cavity was phase-locked to the rotor vibration which verified the link between the pulsation and the rotor vibration. This test suggested that the pulsation being measured in the cavity while the pump was running was also the result of shaft vibration.

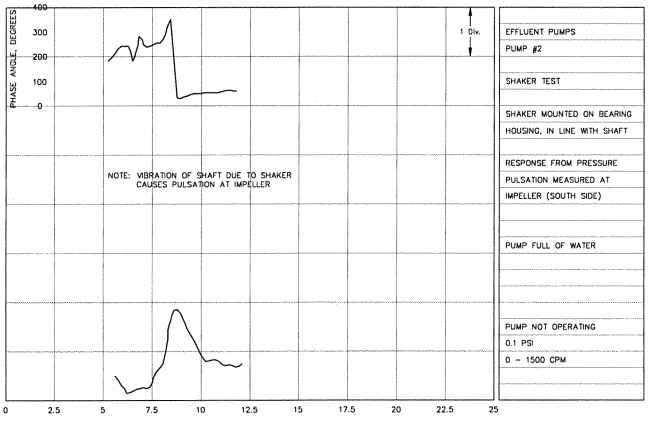

Figure 32. Pulsation Measured Behind Impeller During Shaker Test.

While the pump was operated at low speed with no shaft instability vibration, the shaker tests were repeated in an attempt to excite the rotor instabilities while the unit was operating. Unfortunately, the shaker could not provide enough force to overcome background excitation (flow turbulence, etc.). However, data obtained during a startup indicated that both the backward and forward modes were excited by pulsation generated by the pump at the blade-pass frequency (4× running speed) excitation (Figure 33).

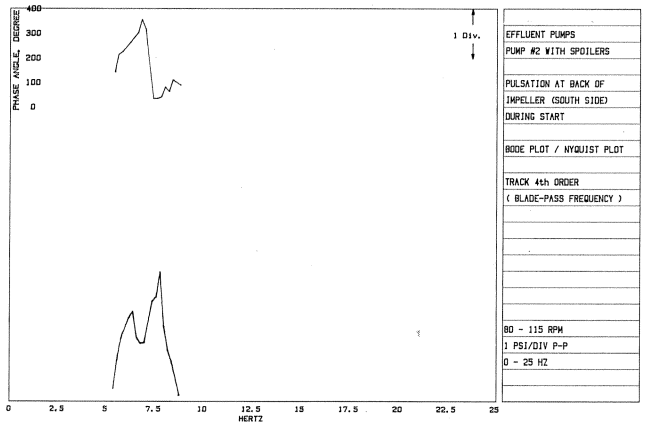

Figure 33. Bodé Plot of Pulsation at Blade-Pass Frequency During Startup.

As shown, the shaker tests provided additional insight into the vibration characteristics of the pump and illustrated that the pulsation at the instability frequencies behind the impeller was created by shaft vibration. The shaker data were also used to normalize the computer model and to estimate the effective stiffnesses of the bearings. Using these data, a rotordynamic analysis was performed to develop a tool to analyze the problem further and to investigate possible modifications.

Rotor Dynamic Stability Analysis

Rotordynamic analyses were done to help identify the source of the problem. The rotor was modelled using shaft dimensions supplied by the manufacturer. Since rolling element bearings were used, the bearing stiffnesses were very high. The bearing support was an upside-down U shape that provided asymmetric stiffness to ground. The computer analysis indicated that using asymmetric stiffness values at the bearing, two distinct instabilities frequencies occurred. Therefore, the bearing pedestal stiffnesses in the X and Y directions were adjusted to normalize the computer model to cause the computed rotor natural frequencies to agree with the frequencies measured during the shaker tests of the dry unit. A ratio of approximately 2-to-1 between the X and Y stiffnesses was required to normalize the model.

Using a finite element approximation of the impeller shape, the water mass in the impeller was computed and added to the rotor model, so that the "wet" rotor natural frequency could be estimated. When this mass was added, the computed lateral natural frequencies agreed with the measured frequency from the shaker test (with wet rotor).

The backward and forward modes were both computed to be at approximately the same frequency until the gyroscopic effects (which would be present when the pump was operating) were included. With these effects added to the computer model, the computed forward and backward supersynchronous instability frequencies agreed well with the measured frequencies.

As stated, the rotor system was marginally stable because the rotor had antifriction bearings that provide little damping. Consequently, the computer analysis indicated that it would be difficult to improve the stability of the rotor system without major modifications to the rotor, or to the bearings.

Field Modifications to Reduce the Destabilizing Forces

Since the stability of the rotor system could not easily be improved, it was decided to try to eliminate the destabilizing forces on the rotor.

Air Injection

It was thought that the cavity behind the impeller could be acting as a bearing or seal, providing destabilizing pressure forces. These destabilizing forces were strong enough to overcome the available damping in the system and caused the rotor to become unstable. Tests were conducted to reduce the effects of the pressure forces in the cavity behind the impeller. Based upon testing by Rudd [10] on similar large pumps and the manufacturers previous experience, air was injected into the cavity which immediately eliminated the supersynchronous vibration. It was thought that the air injection decoupled the fluid from the back side of the impeller shroud, which eliminated the rotating pressure field.

Although the air injection eliminated the instability vibration, it was determined that the air injection was impractical due to operational constraints. Therefore, for this installation, the air injection was not considered to be a solution.

Vents on Ring Cavity

Since the air injection could not be used, other tests were conducted in an effort to reduce the instability vibration. One test was to continuously drain the fluid in the ring cavity by opening several valves that had been installed for the air injection. The vibration data showed that opening the valves had no effect on the vibration.

Increased Wear Ring Clearance

The pump was raised to determine if increasing the clearance between the impeller and the wear ring would affect the instability vibration. The increased clearance also eliminated the possibility that the impeller and the wear ring were rubbing. However, these tests indicated that increasing the wear ring clearance also did not affect the vibration amplitudes at supersynchronous frequencies.

Stationary Spoilers

Eight small stationary ribs ("spoilers") were installed on the pump case in an effort to break up the rotating pressure field behind the impeller (Figure 34). The spoilers were installed without disassembling the pump by bolting them to the housing. Because of space limitations, the height of the spoilers was restricted to approximately 3/8 in. Data obtained with the spoilers indicated that the vibration at the backward mode was attenuated. The differential pressure where the instability occurred was raised from 19 to 25 ft. However, at differential pressures greater than 25 ft, the vibration levels at the backward mode were still excessive. It was felt that the spoilers may have been more effective in reducing the destabilizing forces if their height had been increased and/or if more had been installed.

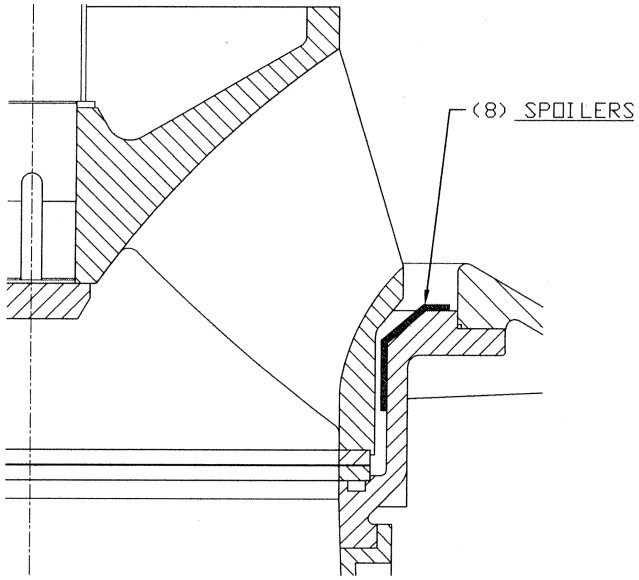

Figure 34. Sketch of Spoiler Installation.

Previous testing by Ohashi, et al. [11], concluded that the forces developed by the impeller increase sharply with decreasing clearances behind the impeller shroud and the housing. Ohashi conducted tests with a spacer with 24 radial grooves, which indicated that the grooves reduced the destabilizing forces by reducing the tangential velocity in the leakage annulus, and thereby reduced the cross coupling stiffness in the same fashion as the stator roughness in a damper seal. It was felt that the stationary ribs also reduced the tangential velocity similar to the grooves. These ribs were also thought to act in a similar fashion to tilting pads in an oil bearing where the pads prevent the oil pressure wave from whirling in the bearing.

Expeller Vanes

The results with the spoilers were encouraging and suggested that the rotor instability problem could possibly be solved if the destabilizing forces acting on the impeller shroud could be reduced. After reviewing previous data and data from tests with other pumps (such as Case I presented here) the manufacturer installed small vanes on the back side of the impeller. It was thought that these "expeller" (pumpout) vanes would reduce the pressure differential developed across the back side of the impeller, thereby reducing the destabilizing forces.

Due to the space limitations, it was difficult to install the pumpout vanes without disassembling the pump. Special vanes were designed that could be bolted to the impeller shroud as shown in Figure 35. The height of the vanes was limited by the available clearances.

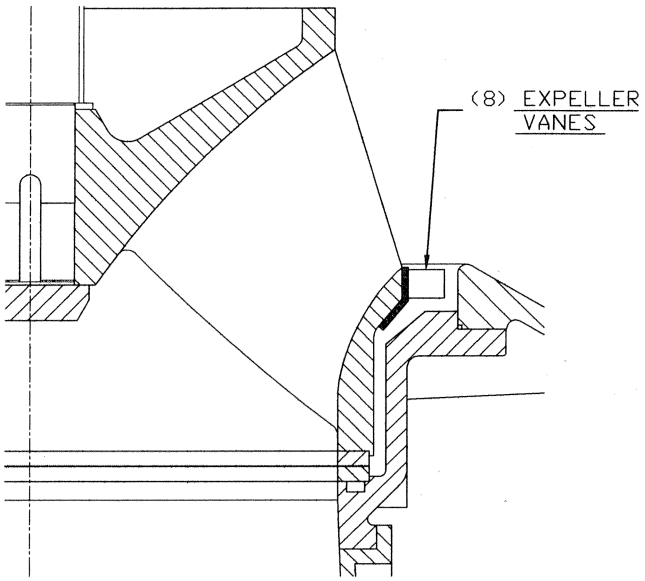

Figure 35. Sketch of Expeller Vane Installation.

After the vanes were installed, field data indicated that the vanes eliminated the instability vibration over the entire operating speed range, even at high discharge pressures. Since the instability vibrations were eliminated, the pumpout vanes were considered to be a permanent modification. There was concern that the bolts attaching the vanes could possibly loosen; however, the pumps have operated for several months without any problems with the vanes. It was recommended that the vanes be welded to the impeller when the pump is disassembled in the future.

CONCLUSIONS

Supersynchronous vibration that was measured was the result of rotor instabilities. The rotors were marginally stable since little damping was provided by the antifriction bearings. Destabilizing forces were provided by fluid in the cavities between the impeller and the pump housing. As shown, these destabilizing forces can result in both forward and backward instability rotor vibration. Since it is difficult to determine if the pulsation in the cavity behind the impeller caused the shaft vibration, or vice versa, two theories have been used to describe the instability phenomenon.

Theory 1: A pressure wave forms in the cavity which has a characteristic frequency. This pressure wave provides forces to the impeller, causing the rotor to vibrate. A reduction in pressure in this area (with pumpout vanes), a reduction in tangential velocity of the fluid (with spoilers), or disturbing the flow with air injection reduces this pulsation wave, thereby reducing the rotor instability. However, this theory does not explain why pulsation would form in the ring cavity at the frequencies experienced, or why the pulsation would propagate in the forward and backward directions.

Theory 2: Cavities behind pump impellers can sometimes act as bearings or seals to produce destabilizing cross coupling forces on

the impellers. The dimensions of the cavity which affect the clearances between the housing and the impellers are important factors in the development and magnitude of the destabilizing forces. It is thought that air injection, spoilers, or pumpout vanes can all diminish cross coupling forces, thereby reducing the rotor instability. Additionally, pumpout vanes can reduce the differential pressure across the cavity which reduces the destabilizing forces. Note that a similar reduction in destabilizing forces results from a reduction in differential pressure across a seal. It is difficult to compute the characteristics of the cross coupling forces in the ring cavity with current computational techniques. Therefore, it is not currently possible to verify this theory analytically.

- Backward rotor instabilities do not necessarily require contact between rotating and stationary components to occur. The data showed that destabilizing pressure forces on the back sides of the impellers were apparently sufficient to initiate both forward and backward supersynchronous shaft instabilities.

- The shaft stability for both horizontal and vertical pumps can be determined using computer models that include the stiffness and damping coefficients for the bearings and the seals. The computer analysis indicated that the horizontal and vertical pumps had low stability (low log dec value), which made them sensitive to the destabilizing effects of the pressure forces behind the impellers.

- The field tests indicated that the actual effective bearing stiffness for antifriction bearings is often less than the quoted stiffness for the bearing alone. The effective bearing stiffness is usually reduced because the bearing is supported by the combined stiffnesses of the bearing housing and pedestal. Furthermore, the stiffnesses may not be symmetrical because of the bearing pedestal geometry.

- Centrifugal pump rotors are often sensitive to the destabilizing effects of the seals (bushings), which can cause the rotor to become unstable and whirl at subsynchronous or supersynchronous frequencies. The analysis and field tests indicated that smooth seals are generally more stable compared to grooved seals. Removing the grooves on the rotating sleeves reduced the destabilizing cross-coupled stiffness (K_{xy} and K_{yx}) and increased the stabilizing direct damping coefficients (C_{xx} and C_{yy}). These effects increased the rotor stability and increased the effective stiffness of the shaft.

- Detailed field measurements are often required to analyze a pump that is experiencing excessive vibration levels. Although it is possible to analyze a system using bearing housing vibration measurements, it is usually better to obtain shaft vibration data. In addition, pulsation data are often required to determine if the instability is a forced instability due to excessive pulsation levels.

SUMMARY

Pumps designed with antifriction bearings have lower damping values, compared to journal bearings, which could influence the stability of the rotor. In these cases, the destabilizing forces acting on the impellers (whatever the cause) can result in excessive rotor vibration at subsynchronous and supersynchronous frequencies. It was shown that the instability vibration can be controlled by increasing the rotor stability to withstand the destabilizing forces acting on the rotor, or by reducing the destabilizing forces.

The tests indicated that air injection, stationary vanes, and expeller or pumpout vanes can be effective in eliminating, or reducing the destabilizing forces acting on the impellers. However, the exact phenomenon causing the destabilizing forces is unknown. Additionally, the exact effects of these elements are not known. Since it is very difficult to quantify these effects, the authors feel that additional analytical and experimental work should be conducted to understand the effects of the pumpout vanes fully.

REFERENCES

1. Pollak, F., *Pump Users' Handbook,* Houston, Texas: Gulf Publishing Company, pp. 31-33 (1980).
2. Karassik, Igor J., et al, *Pump Handbook,* New York, New York: McGraw Hill Book Company, pp. 2.59-2.63 (1986).
3. Lobanoff, Val S. and Ross, Robert R., *Centrifugal Pumps Design & Application,* Houston, Texas: Gulf Publishing Company, pp.345-353 (1992).
4. Smith, D. R. and Wachel, J. C., "Nonsynchronous Forced Vibration in Centrifugal Compressors." Turbomachinery International, pp. 21-24 (January/February 1983).
5. Alford, J. J., "Protecting Turbomachinery from Self-Excited Rotor Whirl," ASME Journal of Engineering for Power, 87, pp. 333-344 (October 1965).
6. Wachel, J. C., "Rotordynamic Instability Field Problem," Second Workshop on Rotordynamic Instability of High Performance Turbomachinery, Turbomachinery Laboratory, Texas A&M University, College Station, Texas (1982).
7. Vance, John M., *Rotordynamics of Turbomachinery,* New York, New York: John Wiley & Sons, Inc, pp. 26-314 (1988).
8. Merovitch, Leonard, *Elements of Vibration Analysis,* New York, New York, McGraw Hill (1975).
9. Scharrer, J. K., "Theory Versus Experiment for the Rotordynamic Coefficients of Labyrinth Gas Seals: Part I A Two Control Volume Model," ASME Transactions Journal of Vibration, Acoustics, Stress, and Reliability in Design, 110, (3), pp. 270-280 (1988).
10. Ruud, F. O., "Vibration of Deriaz Pumps at Dos Amigos Pumping Plant", Source Unknown.
11. Childs, Dara W., *Turbomachinery Rotordynamics: Phenomena, Modeling, & Analysis,* New York, New York: John Wiley & Sons, Inc. (1993).

ACKNOWLEDGMENTS

The authors wish to thank the pump manufacturers for their cooperation in writing this paper and for their permission to present the measured data. The authors also wish to thank the staff of EDI for their assistance in obtaining the data and in preparing the illustrations.